

Interfacial differences between SiO₂ grown on 6H-SiC and on Si(100)

G. G. Jernigan^{a)} and R. E. Stahlbush

Naval Research Laboratory, Code 6810, Washington DC 20375

M. K. Das and J. A. Cooper, Jr.

Department of Electrical and Computer Engineering, Purdue University, West Lafayette, Indiana 47907

L. A. Lipkin

CREE Research, Inc., Durham, North Carolina 27713

(Received 30 October 1998; accepted for publication 12 January 1999)

Oxides grown on *p*-type 6H-SiC and on Si(100) were studied using x-ray photoelectron spectroscopy and sputter depth profiling to determine what differences exist between the two systems. The oxide on SiC is found to be stoichiometric SiO₂, but the oxide is structurally different from the oxide grown on Si(100). We propose that strain introduced during processing accounts for the structural differences. We also found that Si atoms at the SiO₂/SiC interface are chemically different from Si atoms in the bulk of SiC and a number of possible explanations for this are given.

© 1999 American Institute of Physics. [S0003-6951(99)03510-X]

The development of metal-oxide-semiconductor (MOS) structures on silicon carbide substrates is already under way for applications where devices are needed in high temperature or in high power circuits. However, the electrical properties of the oxides grown on SiC do not have the low fixed charge densities (Q_f) and interfacial trapped charge densities (D_{it}) that are obtained for oxides grown on silicon substrates.^{1,2} This is surprising since the oxidation of SiC is expected to result in SiO₂ and volatile carbon monoxide or carbon dioxide gas which should escape. In contrast to Si processing, oxides on SiC are grown in a wet ambient,^{3,4} utilize a postoxidation anneal,^{5,6} and are not improved by hydrogen annealing.¹ Thus, we would like to know what differences exist between the oxides grown on SiC and on Si and how these differences affect the oxide/semiconductor interface.

In this letter we used x-ray photoelectron spectroscopy (XPS) to study two oxides; one grown on a Si terminated *p*-type 6H-SiC and one grown on Si(100) for comparison. XPS is uniquely capable to determine the compositional and chemical nature of the grown oxides by measuring the intensity and energy of the photoelectrons emitted from atoms in the surface. Sputter depth profiling is done to observe how the composition and chemical nature of the atoms change from the oxide to the oxide/substrate interface and into the substrate bulk. We determined the composition of the oxide grown on SiC to be stoichiometric SiO₂, and we did not detect excess carbon in the oxide nor at the interface. We did observe that the resultant oxide has a different chemical environment than the oxide grown on Si. We also discovered that Si atoms in SiC near the interface are different from Si atoms in the bulk of SiC.

The Si terminated 6H-SiC sample was prepared for oxidation by degreasing the sample and followed by a standard RCA cleaning procedure using buffered HF dips. The sample was oxidized in wet O₂ at 1100–1150 °C for ~3 h. The

ambient was switched to Ar, and the sample was cooled to 900–950 °C where it was exposed again to wet O₂ for ~2 h. The sample was immediately removed from the furnace resulting a final oxide thickness of ~50 nm. The electrical characteristics of the grown oxide were determined to be Q_f of $5 \times 10^{11} \text{ cm}^{-2}$ and D_{it} of $1 \times 10^{11} \text{ cm}^{-2} \text{ eV}^{-1}$.⁷ The Si reference sample was prepared by following a standard RCA cleaning procedure. The sample was oxidized at 1000 °C under dry O₂ for 1 h resulting in an oxide ~50 nm thick and having electrical characteristics of $Q_f \leq 5 \times 10^{10} \text{ cm}^{-2}$ and $D_{it} \leq 5 \times 10^{10} \text{ cm}^{-2} \text{ eV}^{-1}$. Each sample was cleaved into 5 × 5 mm squares for XPS analysis and sputter depth profiling.

Sputter depth profiling was done using a 2 keV Ar⁺ ion beam rastered over a 10 mm × 10 mm area. The angle of incidence for the ion beam was ~30°, and a beam current of 0.2 μA was used. This resulted in an effective sputter rate of 0.08 nm/min over such a large area. Under similar conditions, it has been reported that Ar⁺ sputtering results in only a thin amorphous surface layer approximately 1.0 nm thick,⁸ which is much less than the XPS collection depth and does not result in the preferential sputtering of Si or C in SiC.⁹ XPS was performed using Mg x rays ($h\nu = 1253.6 \text{ eV}$). Photoelectrons from Si 2*p*, C 1*s*, and O 1*s* core levels were collected using a hemispherical analyzer with a 50 eV pass energy. An acceptance aperture was used to permit only photoelectrons from a 2 mm × 4 mm area within the sample to be accepted into the analyzer. The choice of sputtering area, sample size, and photoelectron acceptance area were done to assure that there were no edge effects in the XPS measurements.

Figure 1 shows the Si 2*p* spectra for oxidized SiC as a function of sputtering time. Two peaks are clearly seen; Si⁺₄ from the oxide and Si⁺₀ from the SiC substrate. Figure 2 plots the peak areas of Si⁺₄ and Si⁺₀ as well as the C 1*s* and O 1*s* peak areas as a function of sputtering time. We observe that the Si⁺₄ and O 1*s* peak area ratio is constant in the oxide. The Si⁺₄ to O 1*s* ratio for the oxide grown on SiC was 4.6 and is identical to the ratio found for the oxide grown on Si(100). Correcting for the different experimental

^{a)}Electronic mail: glenn.jernigan@nrl.navy.mil

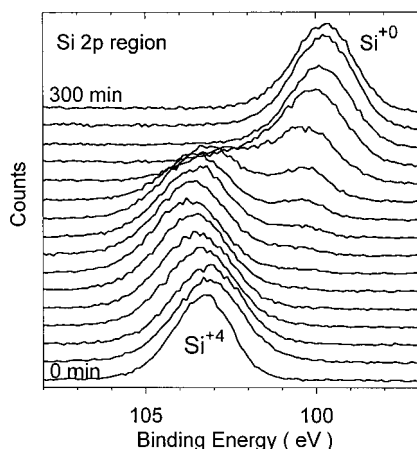


FIG. 1. XPS Si 2*p* spectra of SiO₂ grown on 6H-SiC taken after each 20 min sputtering interval from 0 to 300 min (upward). The Si⁺⁴ peak is from the oxide and the Si⁺⁰ peak is from the substrate.

cross sections of the Si 2*p* and O 1*s*, this ratio is equivalent to a Si to O stoichiometry of 1 to 2. At the interface between SiO₂ and SiC, we observe a decrease in the Si⁺⁴ and O 1*s* peaks and a rise in the Si⁺⁰ and C 1*s* peaks. While not immediately obvious in the figure, the ratio of Si⁺⁰ to C 1*s* decreases initially and becomes constant at a value of 1.4 for bulk SiC. XPS has a longer sampling depth for the Si⁺⁰ photoelectron as compared to the C 1*s* photoelectron and this may account for a larger initial Si signal. The width of the transition from oxide to SiC is due to the escape depth of the photoelectrons, and the actual interface may be atomically abrupt. It has been proposed that excess C can be found at the interface.¹⁰ We did not observe any excess carbon but we have a limiting sensitivity of 0.1 monolayers due to the underlying of the bulk C signal. C was also not detected inside the oxide layer, but it may have been present below the bulk XPS sensitivity limit of 0.5%. Sputter depth profiling shows no difference in stoichiometry for an oxide grown on SiC as compared to an oxide grown on Si(100), however the local environment of the Si atoms in the oxide and in the substrate near the interface is not the same.

Figure 3 shows the binding energy of the Si⁺⁴ and Si⁺⁰ peaks for the oxide on SiC and on Si(100) as a function of sputtering time. We observe two distinct differences. First,

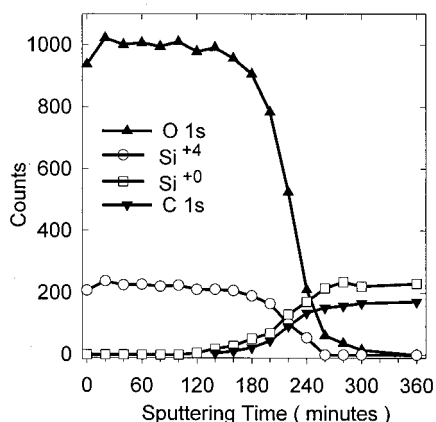


FIG. 2. XPS peak areas for Si⁺⁴, Si⁺⁰, O 1*s*, and C 1*s* as a function of sputtering time for SiO₂ grown on 6H-SiC.

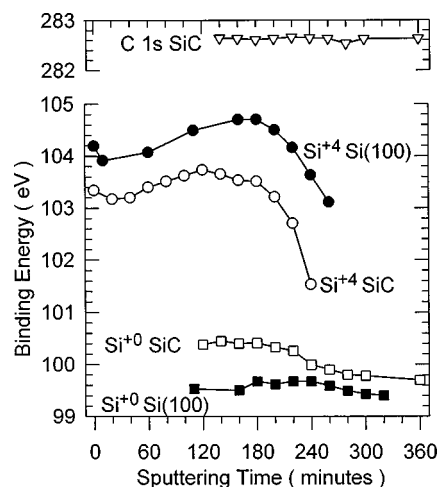


FIG. 3. XPS binding energy for Si⁺⁴, Si⁺⁰, and C 1*s* as a function of sputtering time for SiO₂ grown on 6H-SiC and on Si(100).

the Si⁺⁴ binding energy is consistently lower for the oxide grown on SiC. Second, the Si⁺⁰ binding energy for SiC shifts to lower energies through the interfacial region but the Si(100) sample does not shift. The shift is not the result of a Si suboxide species. In cases where suboxides have been observed, the suboxide is seen as a small shoulder at a higher binding energy from a much larger Si⁺⁰ peak, and the presence of suboxide peaks does not cause a change in the position of the Si⁺⁰ peak. The change in binding energy for the Si⁺⁴ peaks through the interfacial region is similar for both SiC and Si(100) and has been previously reported for the SiO₂/Si interface.¹¹ Not shown in Fig. 3 are the changes in the O 1*s* binding energy for SiO₂ on SiC and on Si(100) as a function of sputtering time, because the O 1*s* peak shifts in synchronization with the Si⁺⁴ peak. The difference in binding energy between O 1*s* and Si⁺⁴ is a constant and is the same value within experimental error for SiC and Si(100).

The lower Si⁺⁴ binding energy in SiO₂ grown on SiC when compared to Si(100) is most likely due to a structural difference between the oxides. Because the Si⁺⁴ to O 1*s* ratio remains constant in the oxide and is identical to the ratio found for the Si(100), we can rule out the possibility that the binding energy is lower due to the formation of a sub-stoichiometric oxide. Another possible explanation that we also discount would be the incorporation of another element into the oxide. We have already mentioned that carbon was not found in the oxide, and if another element were present, it would have to be present in observable amounts to cause such a significant shift in the Si⁺⁴ binding energy. Additionally, the element would have to appear more electron donating to lower the binding energy of Si⁺⁴. In support of our assignment of a structural difference, it has been recently reported that the Si⁺⁴ peak from a stoichiometric oxide can be shifted to a higher binding energy by compressively stressing it with hydrogen implantation.¹² In our case, the oxide binding energy for SiC was found to be less than the standard value of 104 eV for stoichiometric oxide on Si, indicating that the structural difference could be due to tensile strain in the oxide film. The differences in strain may be caused by thermal stress differences among Si, SiC, and SiO₂, which have been proposed as an explanation for dif-

ferences in fixed charge and interfacial trap density as a function of processing conditions.¹³ Additionally, strain in the oxide could be the result of the evolution of gaseous CO or CO₂ through the oxide or could result from the increased lattice distance between Si atoms in SiC as compared to Si(100).

The change in the binding energy for Si⁺ of SiC is an interesting and unexpected result. The Si⁺ peak is observed to be shifting through the interface. The Si⁺ peak is seen before all of the oxide has been sputter removed, because the Si⁺ photoelectron has an inelastic mean free path in the oxide of ~4.6 nm and is first visible at a distance of 14 nm above the interface. Similarly, the C 1s peak can also be first seen when the oxide is thinned to 10 nm. In Fig. 3, we also plotted the C 1s binding energies as a function of sputter time through the interfacial region. We observe that the C 1s peak does not change in energy. Because the C 1s peak acts differently from the Si⁺, this is an indication that the cause for the Si⁺ shift is localized to Si atoms at the interface. The cause of the shift cannot be discerned from this work and additional studies are planned, but there are a few plausible explanations which can be proposed. First, Si atoms at the interface may be under stress in a manner similar to what we proposed to explain the lower Si⁺ binding energy of the oxide. The oxide is grown on SiC through the adsorption of O onto Si and then O is inserted into the back bond between Si and C.¹⁴ The substitution of an O atom for a smaller C atom in the interface or the need for O to bridge a longer distance between Si atoms as compared to Si(100) may lead to stress. Second, there may be trapped CO bound to Si at the interface¹⁵ which perturbs the Si⁺ binding energy. CO has a strong dipole moment which may induce an electrostatic interaction. We do not observe extra peaks for C 1s and O 1s in the XPS from CO, but they may be small and hard to observe next to the bulk signals. Third, there may be an oxycarbide layer.^{16,17} An oxycarbide layer may contain only Si-O-Si bridges and may not contain Si-O-C bridges, thus producing a shift solely in the Si atoms. Fourth, the oxidation process may remove C from the lattice creating vacancies or a Si rich region between the oxide and the SiC bulk. We did observe a higher Si⁺ to C 1s ratio initially at the interface which could be due to excess Si or to a difference in XPS sampling depth. Finally, there may be other elements, in minor amounts, which we did not detect that could cause the shift.¹⁸ Hydrogen, in particular, from the wet oxidation could be present but undetectable by XPS.

Differences between an oxide grown on 6H-SiC and an oxide grown on Si(100) were sought to explain the reported differences for the electronic properties of MOS structures made in each material. We found that the oxidation of SiC does result in the formation of a stoichiometric SiO₂ layer but that the chemical environment of the SiO₂ layer is different from the SiO₂ layer which was grown on Si(100). The difference between the two SiO₂ layers was proposed to be structural in nature and resulting from strain in the oxide grown on SiC. No excess carbon was detected in the oxide or at the interface. We found that there was a change in the chemistry of Si atoms at the interface of SiC. Si atoms at the interface were found to be in a different environment from atoms in the bulk of SiC and a number of possible explanations were discussed.

This work was supported by the Power Electronics Building Blocks program monitored by Dr. George J. Campisi of the Office of Naval Research.

¹M. R. Melloch and J. A. Cooper, Jr., MRS Bull. **22**, 42 (1997).

²D. Alok, P. K. McLarty, and B. J. Baliga, Appl. Phys. Lett. **64**, 2845 (1994).

³D. Alok, P. K. McLarty, and B. J. Baliga, Appl. Phys. Lett. **65**, 2177 (1994).

⁴S. Zaima, K. Onoda, Y. Koide, and Y. Yasuda, J. Appl. Phys. **68**, 6304 (1990).

⁵L. A. Lipkin and J. W. Palmour, J. Electron. Mater. **25**, 909 (1996).

⁶J. N. Shenoy, J. A. Cooper, and M. R. Melloch, Appl. Phys. Lett. **68**, 803 (1996).

⁷M. K. Das, J. A. Cooper, Jr., and M. K. Melloch, J. Electron. Mater. **27**, 353 (1998).

⁸E. Paparazzo, M. Fanfoni, and E. Severini, Appl. Surf. Sci. **56-58**, 866 (1992).

⁹M. J. Bozack, Phys. Status Solidi B **202**, 549 (1997).

¹⁰V. V. Afanas'ev, M. Bassler, G. Pensl, M. J. Schulz, and E. S. von Kaminski, J. Appl. Phys. **79**, 3108 (1996).

¹¹F. J. Grunthaner and P. J. Grunthaner, Mater. Sci. Rep. **1**, 65 (1986).

¹²P. J. McMarr, B. J. Mrstik, R. K. Lawrence, and G. G. Jernigan, IEEE Trans. Nucl. Sci. **44**, 2115 (1997).

¹³W. Xie, J. N. Shenoy, S. T. Sheppard, M. R. Melloch, and J. A. Cooper, Jr., Appl. Phys. Lett. **68**, 2231 (1996).

¹⁴V. M. Bermudez, J. Appl. Phys. **66**, 6084 (1989).

¹⁵H. Tsuchida, I. Kamata, and K. Izumi, Jpn. J. Appl. Phys., Part 1 **34**, 6003 (1995).

¹⁶C. Öneby and C. G. Pantano, J. Vac. Sci. Technol. A **15**, 1597 (1997).

¹⁷B. Hornetz, H.-J. Michel, and J. Halbritter, J. Mater. Res. **9**, 3088 (1994).

¹⁸S. Sridevan, P. K. McLarty, and B. J. Baliga, IEEE Electron Device Lett. **17**, 136 (1996).